Nephrol Dial Transplant (2007) 1 of 10
doi:10.1093/ndt/gfm587

NDT
Nephrology Dialysis Transplantation

Original Article

Urinary proteome and potential biomarkers associated with serial pathogenesis steps of focal segmental glomerulosclerosis

Hao-Ai Shui[1], Tzu-Hao Huang[1,2], Shuk-Man Ka[3], Pei-Hsiu Chen[4], Yuh-Feng Lin[5] and Ann Chen[3]

[1]Graduate Institute of Medical Sciences, National Defense Medical Center, Taipei, [2]Department of Nursing, Chang-Gung Institute of Technology, Taoyuan, [3]Department of Pathology, Tri-Service General Hospital, [4]Graduate Institute of Life Sciences and [5]Department of Internal Medicine, Tri-Service General Hospital, National Defense Medical Center, Taipei, Taiwan, R.O.C.

Abstract

Background. Focal segmental glomerulosclerosis (FSGS) is a chronic nephropathy showing characteristic glomerular sclerosis. So far, the diagnosis and prognosis of FSGS rely mainly on the invasive biopsy. Searching for potential FSGS-associated urinary biomarkers representing pre-sclerotic and serial sclerotic stages of FSGS could be helpful to the non-invasive diagnosis and prognosis of FSGS.

Methods. In the present study, we used a 2D gel-based proteomic approach to identify urinary proteins at pre-sclerotic and different sclerotic stages of an FSGS mouse model in order to find FSGS-related urinary proteins. The FSGS mouse model was established in Balb/c mice by a single injection of adriamycin, and disease severity was monitored by renal biological parameters and histopathological features. Urine was collected on days 0, 4, 7, 11, 15 and 20, and subjected to two-dimensional electrophoresis (2-DE) analysis. Proteins were identified by matrix-assisted laser desorption ionization/time of flight mass spectrometry (MALDI-TOF MS) and a protein database search. Some of the identified proteins were confirmed by western blot analysis.

Results. We identified 37 urinary proteins showing characteristic patterns of dynamic changes along the disease course of FSGS. Early urinary proteins appearing before glomerular scleoris were noticed. Importantly, 11 urine proteins are novel to FSGS and have known functions highly associated with different pathogenetic steps of the disease, including haemodynamic disturbance, podocyte apoptosis, ECM-protein deposition and glomerular sclerosis.

Conclusions. Some urinary proteins appearing earlier than glomerular sclerosis could serve as potential early diagnostic biomarkers. The proteins with the pathogenic roles could serve as potential non-invasive prognostic markers of FSGS, and give an insight into pathogenic mechanisms of this sclerosis disease.

Keywords: diagnosis; focal segmental glomerulosclerosis; potential urinary biomarkers; prognosis; proteomics

Introduction

Focal segmental glomerulosclerosis (FSGS) is a chronic glomerular nephropathy showing the pathohistological feature of sclerosis in some glomeruli (focal) in which only part of a glomerular capillary tuft is affected (segmental). It is caused by a wide range of factors, including environmental toxins, genetic factors, infectious agents, haemodynamic problems, or other types of nephritis [1]. Clinically, FSGS is classified as a type of nephrotic syndrome, which is characterized by massive proteinuria without substantial nephritic features. Microscopically, the first glomerular cell to be affected in FSGS is the podocyte (glomerular visceral epithelial cells) that could be damaged by the pathogenic factors, leading to breakdown of the renal filtration barrier, and thus leakage of blood and tissue proteins into the urine [1–3]. So far, diagnosis of FSGS still relies on biopsy. Identification of the urinary proteins in FSGS animal models would be helpful to uncovering the potential proteins for non-invasive diagnosis and prognosis of FSGS.

Proteomic approaches have been widely used to simultaneously study the expression of many proteins (rather than individual proteins) in a biological sample, and have been applied to the identification of potential nephropathy-associated biomarkers [4–11]. However, despite some advances made by proteomic analyses of tissue and urine in animals and patients [3,11], novel biomarkers for improving the diagnosis and

Correspondence to: Dr Hao-Ai Shui, Graduate Institute of Medical Sciences, National Defense Medical Center, 161, Min-Chuan East Road, 6th Section, Taipei, Taiwan (114), ROC.
Email: haoai@ndmctsgh.edu.tw

prognosis of FSGS are still lacking. In addition, although a urinary biomarker is more valuable than a tissue biomarker for clinical use in terms of non-invasiveness of diagnosis, urinary biomarkers that can represent different sclerotic stages of FSGS remain unclear. Analysing the urinary proteome at different stages of the disease (including the early and pre-sclerotic stage) could be helpful to identifying potential proteins to serve as FSGS-related urinary biomarkers. This approach has been applied to minimal change disease and membranous glomerulonephropathy [5,10].

Some mechanisms underlying the pathogenesis of FSGS have been revealed, which include abnormal metabolism of extracellular matrix (ECM) proteins, imbalance of sclerotic and anti-sclerotic factors, disturbed glomerular haemodynamics, and oxidative stress-induced damage and apoptosis of glomerular cells. These result in damage to the podocytes, rupture of the renal filtration barrier, severe proteinuria and glomerular sclerosis [2,12,13]. We have established an FSGS animal model in Balb/c mice by a single injection of adriamycin (AD) [14–16], and identified some FSGS-associated biomarkers using the model by traditional biochemical approaches [15,16]. In the present study, we further used proteomic technologies established in our labs [17] to examine serial changes of the urinary proteome in the same animal model. Our aim is to identify novel urinary proteins associated with the pathogenesis of FSGS which have potential to serve as non-invasive biomarkers for diagnosis and prognosis of the disease.

Subjects and methods

Animals, drug treatment and sample collections

The experiments were performed on 8-week-old BALB/c mice. The mice were injected intravenously with a single dose of AD (0.1 mg/10 g body weight) or normal saline ($n = 6$) as described previously [15,16]. The six saline-injected animals were used as normal controls, and their urine and blood were collected every day for repeated biochemical analyses, and kidneys harvested on day 20 for histological examinations. Since our previous study demonstrated that AD-treated mice show different severities of proteinuria and glomerular sclerosis on days 0, 4, 7, 11, 15 and 20, these days were chosen for collection of blood and urine samples and sacrifice of the animals to harvest the kidneys for histology. As our previous studies have demonstrated that there is no difference between levels of saline-treated mice (days 0–20) and basal levels (day 0) of AD-injected mice in various biochemical and histological parameters [14–16], the basal levels (day 0) of AD-injected mice ($n = 6$) were used as the statistical control for ANOVA comparisons with the AD-induced FSGS mice on days 4, 7, 11, 15 and 20 ($n = 6$ for each day). Blood was collected through the retro-orbital venous plexus [15,16]. For avoiding contamination by food, water and faeces that can happen using metabolic cages, mouse urine was obtained by gentle bladder massage and collected on a Parafilm film. In order to prevent protein degradation, a proteinase inhibitors cocktail (Sigma P8340) was added to the urine. Serum creatinine, blood urea nitrogen (BUN) and urine protein concentration were measured on days 0, 4, 7, 11, 15 and 20 after AD treatment.

Measurement of serum creatinine, blood urea nitrogen and urine protein concentration

Samples of serum or urine were microfuged and stored in liquid nitrogen until analysed. Unlike our previous publications [15,16], a modified Bradford method that can prevent interference from urea in urine, was used to measure urinary protein concentration (milligram per decilitre) [18]. Urine protein concentrations were then calibrated by urine creatinine concentrations. Serum creatinine was measured using a picric acid colorimetric kit (Sigma 555-1) and BUN was measured using a urease assay kit (Sigma 640-5) as described previously [19].

Histopathology

Renal tissues were fixed in 10% buffered formalin for routine histopathological evaluation. The paraffin-fixed renal sections were immersed in xylene to remove paraffin, rehydrated in graded ethanol, stained with haematoxylin and eosin (HE), and examined using a light microscope (Olympus, Tokoyo, Japan). Semi-quantification of sclerosis was performed dependent on morphological changes on a scale of 1–4, as described previously [15,16].

Desalting and concentration of urine samples

The urine collected by bladder massage was desalted and concentrated by ultrafiltration, which has been confirmed by our preliminary data (data not shown) and demonstrated by a previously published paper [20] to be able to recover most of urinary proteins in comparison with other methods such as acetone precipitation [10]. In terms of mouse urine, protein loss due to precipitation or degradation was not detected during the ultrafiltration process, while a significant loss of urinary proteins can be observed using precipitation methods (data not shown).

Briefly, fresh urine was forced through the Microcone (Millipore, MA, USA) by centrifugation at 10 000 *g* at 4°C for 1 h. The proteins retained on the upper surface of the Microcone membrane were washed twice, and the retained urinary proteins dissolved with lysis buffer (9 M urea, 2% CHAPS, 1% DTT, and 0.5% IPG buffer pH 3–10) by gentle shaking for 15 min.

2-DE

Urinary proteins (250 µg) from the AD-treated mice (days 0–20) were loaded onto an IPG strip (Immobiline DryStrip 3–10, GE Healthcare, NJ, USA) for simultaneous rehydration. Isoelectric focusing (IEF) was performed using the voltage-time programme of 50 V for 12 h, 500 V for 1 h, 1000 V for 1 h and 8000 V to give a total of 80 000 V h, which was modified from our original programme to optimize separating the urinary proteins [17].

Immediately after focusing, the IPG strips were sealed in plastic holders and stored at −20°C. Prior to SDS-PAGE, the strips were equilibrated for 15 min in equilibration buffer

(6 M urea, 2% SDS, 50 mM Tris, pH 8.4, 30% glycerol) containing 1% DTT, then for 15 min in equilibration buffer containing 2.5% iodoacetamide. The second dimension separation was run using a vertical electrophoresis system (GE Healthcare, NJ, USA) in 1 mm 12.5% gels at 20 mA/gel at 15°C. After electrophoresis, the gels were fixed and stained using a protocol in our previous paper [17]. The spots were then digested with trypsin and subjected to direct mass spectrometry (MS) protein identification.

Spot detection, quantification and comparisons

Two D gel analysis software (ImageMaster 2D platinum, GE Healthcare, NJ, USA) was used for spot detection, gel matching and spot quantification. For evaluating the percent amount of a protein in urine, the relative volume (percent spot volume; PSV) of each protein on a 2D gel was evaluated by the software using the formula: PSV = (spot volume/total volume of all spots) × 100%. In addition, to compare protein levels between different urine samples with different protein and creatinine concentrations, the concentration of each protein was calculated and normalized to the corresponding concentration of urine creatinine using the equation: Normalized protein level (NPL) = (PSV × total protein concentration)/creatinine concentration. Repeated measure ANOVA and Newman–Keuls test was used to compare the NPL of basal levels (day 0) with those of FSGS mice (days 4–20). Spots that showed significant difference in protein levels between the groups were selected for protein identification.

Digestion of proteins and MALDI-TOF MS

All protein spots of interest were manually excised and subjected to in-gel digestion using a protocol in our previous publication [17]. The mass spectrometer used for protein analysis was a Bruker Biflex IV MADLI-TOF MS (Bruker Daltonics, Bremen, Germany). To obtain the peptide mass fingerprint (PMF), each mass spectrum was averaged from signals generated from 500 laser shots. The mass spectra were processed using Flexanalysis™ and Biotools™ software (Bruker Daltonics, Bremen, Germany) and the data subjected to a search against the UniProt database (http://www.pir.uniprot.org) by the MS-Fit database searching engine (http://prospector.ucsf.edu/ucsfhtml4.0/msfit.htm). For each PMF search, the mass tolerance was set to 100 p.p.m. and one missed tryptic cleavage was allowed.

Western blot analysis

Urine (10 µl) from AD-treated mice (days 0–20) was subjected to 10% SDS-PAGE. Proteins were then transferred to a Hybond PVDF membrane (GE Healthcare, NJ, USA). The membranes were blocked for 1 h at room temperature in 15 ml of blocking buffer [Tris-buffered saline, pH 8.0, containing 0.05% Tween-20 (TBST) and 5% skimmed milk], and then incubated with rabbit anti-collagen IV antibody (Santa Cruz Biotechnology, Santa Cruz,. CA, USA), mouse anti-glutathione s-transferase antibody (Abcam, Cambridge, UK) and mouse anti-cadherin antibody (Abcam, Cambridge, UK) for 1 h at room temperature, then washed three times with TBST, followed by incubation with the appropriate secondary antibody (1 h at room temperature). The proteins on the membrane were visualized with an ECL detection kit (Millipore, Bedford, MA, USA), and protein intensities quantified by a densitometer. Data were presented as the ratio of densities of the proteins to creatinine concentrations of urine.

Statistics

All data are presented as the mean ± SEM. Statistical analysis was performed using repeated measures analysis of variance (ANOVA). A Newman–Keuls test was carried out when the ANOVA comparisons gave a significant result. Differences were considered significant at $P < 0.05$.

Results

Renal biological parameters

Proteinuria was evaluated in the AD-injected mice. Compared to basal levels (1.10 ± 0.13), the creatinine-corrected urine protein levels were significantly increased on day 7 (40.4 ± 1.38) ($F = 26.7$, $P < 0.05$) and remained high throughout the experiment (Figure 1A). BUN and serum creatinine, two parameters for evaluating renal function, were also examined. The former showed a significant and persistent elevation from day 11 (39.1 ± 2.0 mg/dl compared to basal levels of 21.7 ± 0.8 mg/dl; $F = 116.4$, $P < 0.05$) (Figure 1B), and the latter also showed a significant increase from day 11 (1.31 ± 0.09 mg/dl vs. 0.52 ± 0.01 mg/dl; $F = 62.57$, $P < 0.05$) (Figure 1C).

Glomerular sclerosis in the FSGS model

To confirm the establishment of the FSGS model, histopathological examination was performed on kidney sections obtained at different time points. As shown in Figure 2A, expansion of the ECM and deposition of hyaline mass in the glomeruli were occasionally seen on day 7, and became statistically significant from day 11 (22.5 ± 1.5 compared to basal levels of 0.0 ± 0.0; $F = 125.9$, $P < 0.05$) (Figure 2B). The extent of sclerosis correlated well with the severity of the renal biological parameters shown in Figure 1.

Serial changes in the urinary proteome in FSGS

The 2D gel pattern for the basal-level mice (day 0) was markedly different from those for the FSGS mice on days 4–20 (Figure 3). The serial changes in the urinary proteome of the AD-treated mice are shown in Figure 3. The most dramatic change occurred between days 0 and 4, while, after day 4, the 2D gel patterns were similar, but exhibited dramatic changes in the expression of each individual protein. In all, 37 urinary proteins that were up- or down-regulated in the diseased mice compared with the basal-level mice (Figure 4) were identified; the characteristics of these spots are shown in Table 1. The proteins that demonstrated a serial change in relative amount are

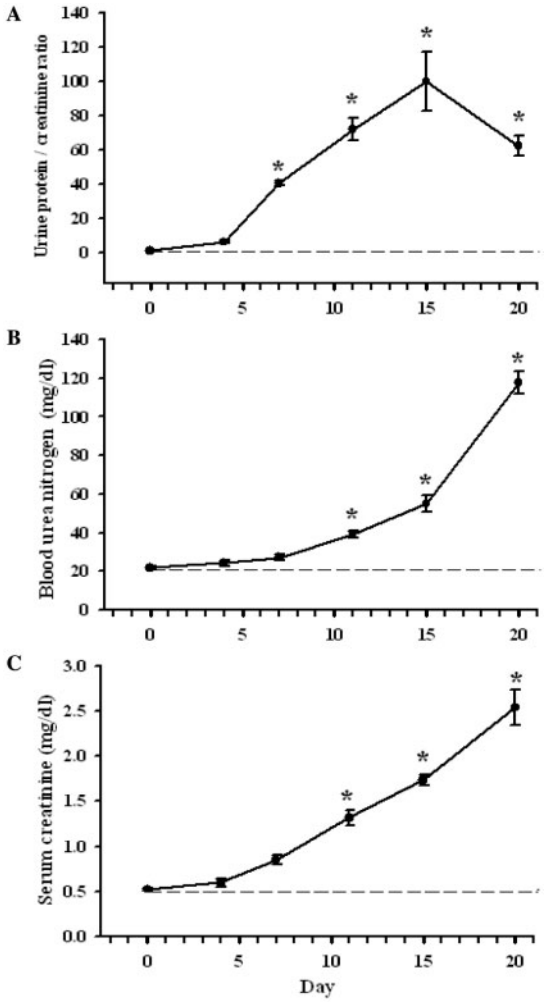

Fig. 1. Renal biological parameters in AD-treated mice. Three typical parameters for evaluation of renal function, (**A**) urine protein, (**B**) BUN and (**C**) serum creatinine, were measured at various time points after AD treatment. $n = 6$ for each day, $^{*}P < 0.05$ compared to day 0. The dashed lines show the mean value for mice treated with saline.

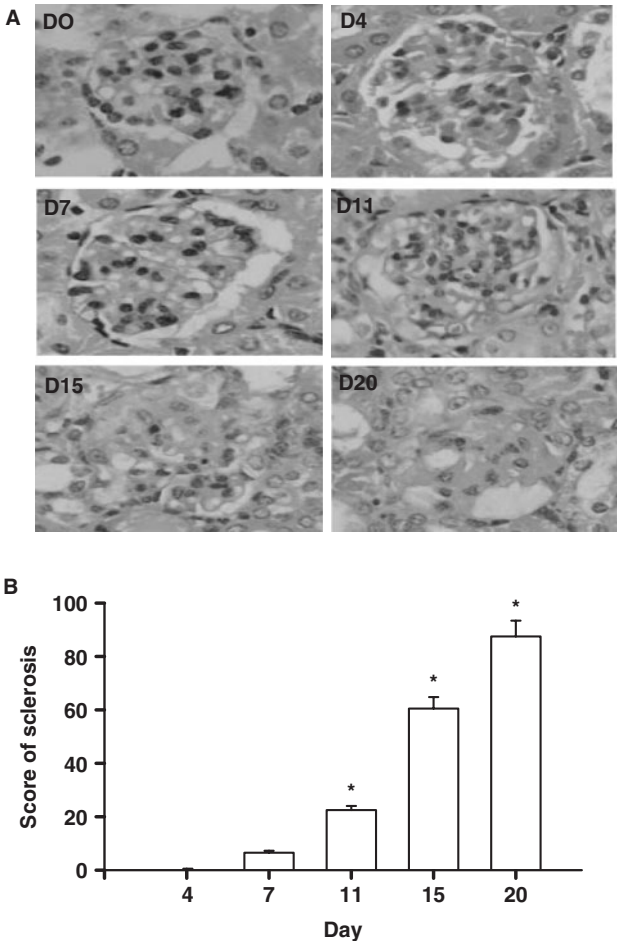

Fig. 2. Glomerular histopathology in AD-treated FSGS mice. (**A**) Kidney tissue on day 0, 4, 7, 11, 15 or 20, showing a gradual increase in the collapse of the glomerular tufts, together with increased segmental sclerosis in the glomeruli. Haematoxylin and Eosin staining. Original magnification, 400×. (**B**) Semi-quantitative plot showing the sclerosis scores for the glomeruli in tissue sections. The sclerosis scores were calculated as described in the 'Subjects and methods' section. $n = 6$ for each day, $^{*}P < 0.05$ compared to day 0.

shown in Figure 5; their PSV and NPL, calculated as described in the 'Subjects and methods' section, are also given to help compare creatinine-calibrated protein levels across different urine samples. The creatinine-calibrated levels of three identified proteins were confirmed by western blots shown in Figure 6.

Proteins with potential as early diagnostic biomarkers of FSGS

Marked proteinuria appeared on day 7, which is earlier than the significant onset of glomerular sclerosis on day 11 (Figure 1A *vs*. Figure 2B). Since sclerosis of glomeruli is the key determinant of FSGS [1,2], the proteins that appeared in the urine before the onset of glomerular sclerosis (day 7) have higher diagnostic values as early biomarkers than those appearing after the onset (days 7–20). These potential early biomarkers are highlighted in Table 1.

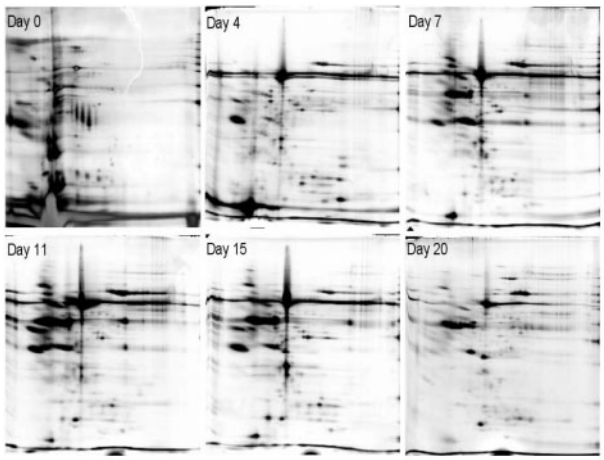

Fig. 3. Representive urinary proteome profiles of AD-induced FSGS mice at different time points of disease. Urinary proteins were separated on a pH 3–10 IPG strip in the first dimension and on an SDS–polyacrylamide (12.5%) gel in the second dimension.

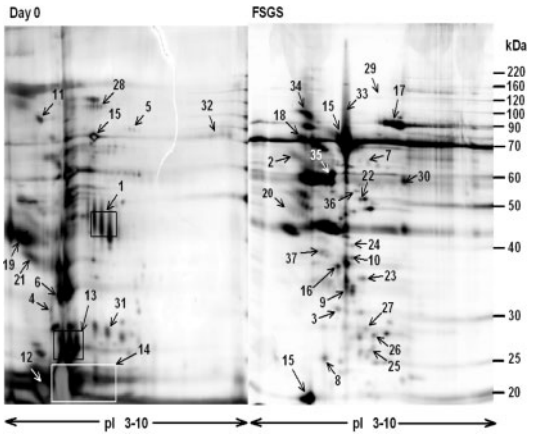

Fig. 4. Representative 2D gel maps for day 0 and FSGS mice. The sample for the FSGS mice was collected on day 7, when most of the urinary proteins can be detected on a 2D gel. The molecular weight and p*I* ranges are indicated, respectively, at the right and bottom of each gel. The identified proteins are indicated by spot numbers which are the same as those shown in Table 1. The boxes enclose spots assigned to the same protein.

Proteins with potential to affect glomerular sclerosis

Glomerular sclerosis, which is caused by the gradual deposition of ECM proteins [15], is a hallmark of FSGS. Two ECM proteins, the collagen fragment (spot 1) and ECM protein 1 (ECM 1, spot 2), were unequivocally identified (Table 1), showing down-regulation and up-regulation respectively in urine of FSGS mice (Figure 5). Bone morphogenetic protein (BMP)-7, a member of the transforming growth factor (TGF-β) family, can counteract the glomerular sclerosis by suppressing SMAD signalling [21]. However, two novel BMP-binding proteins which suppress BMP activities, the cerberus (spot 3, Table 1) and tomoregulin fragment (spot 4, Table 1), were detected in mice urine; cerberus showed up-regulation, while tomoregulin fragment showed down-regulation, in urine of diseased mice (Figure 5). Proteinases that degrade ECM proteins can also counteract glomerular sclerosis. ADAM 32 (spot 5, Table 1), a novel member of the 'a disintegrin and metalloprotease domain (ADAM)'

Table 1. Identified proteins

Spot no.	Early protein	Accession no.	Protein	Theoretical *Mr*/p*I*	Observed *Mr*/p*I*	No. of matching peptides	Sequence coverage (%)
1		Q6PHB5	Collagen IV (Fragment)	49.8/8.5	45/6	10	44.6
2	□	Q61508	Extracellular matrix protein 1	63/6.3	68/4.4	14	29.3
3	□	O55233	Cerberus	30.4/8	32/5.6	10	41.5
4		Q9JJS1	Tomoregulin-1 (Fragment)	38.2/6.4	37/5.8	23	61.0
5	□	Q8K410	ADAM 32	83.6/6.8	80/6.9	13	30.9
6		P15947	Renal kallikrein	36/5.1	32/5	6	31.0
7	□	O08677	Kininogen-1 precursor	73.1/6.1	66/6.5	19	31.8
8	□	P10649	Glutathione s-transferase	25.8/8.1	29/6.6	10	53.0
9	□	Q8CHZ2	Apoptosis-inducing factor-2	36.6/7.1	34/5.8	22	54.7
10	□	P10107	Annexin A1	38.6/7.1	36/6.1	17	43.2
11		P09803	E-cadherin	98/4.7	100/4.3	22	30.9
12		P11588	Major urinary protein 1	20/5	19/9.9	17	67.8
13		P11589	Major urinary protein 2	20.6/5	27/4.7	10	63.9
14		Q5D068	Major urinary protein 3	21/4.7	21/4.5	24	77.7
15	□	P07724	Albumin	68.7/5.7	70/5.8	24	38.2
16		Q8CG74	Albumin (Fragment)	23.6/5.5	37/6.2	7	32.3
17	□	Q921I1	Serotransferrin	78.8/7.2	90/7.3	43	64.4
18	□	P23953	Carboxylesterase N	61.1/5.1	70/4.6	29	32.7
19		Q8BTL3	Vacuolar proton pump D subunit	40.2/5.1	40/3.8	7	31.3
20		P81105	α-1-Antitrypsin	45.8/5.3	49/4.2	9	30.3
21		O35887	Crocalbin	37/4.5	37/4	20	60.0
22	□	Q8K566	Cysteine sulfinic acid decarboxylase	55.1/6.2	52/6.2	14	33.3
23		Q9JII6	Aldehyde reductase	36.4/6.9	35/6.3	18	54.3
24	□	Q9JLH8	Tropomodulin-4	39.2/4.8	40/6	15	24.9
25	□	Q8R3U8	Sorbitol dehydrogenase 1	21/7.9	26/6.5	15	71.3
26	□	P23506	Protein-β-aspartate methyltransferase	24.5/7.3	27/6.6	7	33.6
27		Q9R0P3	Esterase D	31.3/6.7	28/6.4	14	64.2
28		Q80XQ2	TBC1 domain family member 5	91.8/6.3	97/5.9	10	18.3
29		P16283	Anion exchange protein 3	135.1/5.9	132/6.7	16	20.4
30		Q9WVS5	TCP-1 containing chaperonin	59.5/5.4	58/7.5	29	53.2
31		Q3UMV5	Plasma retinol-binding protein	23.2/5.7	28/6.2	11	57.2
32		Q8BME3	clone:6720429F19	81.5/9.6	76/9.6	27	45.5
33		P27546	Microtubule-associated protein 4	117/4.9	120/5.8	17	21.3
34		P16406	Glutamyl aminopeptidase	107.9/5.3	102/4.7	22	17.6
35		P60670	Nuclear protein localization 4	67.8/6	61/5.4	16	34.8
36	□	Q3TIY6	Rab GDP dissociation inhibitor	50.6/5.9	55/6.1	17	43.1
37		Q8BTH1	Fatty acid hydroxylase	42.9/6.8	37/5.2	8	22.8

Potential early FSGS biomarkers are highlighted. The accession number and the name in the UniProt database for each protein are shown, followed by the theoretical and observed molecular mass (*Mr*) and the isoelectric point (p*I*). The number of matching peptides and sequence coverage were calculated using Biotools^{TM} software.

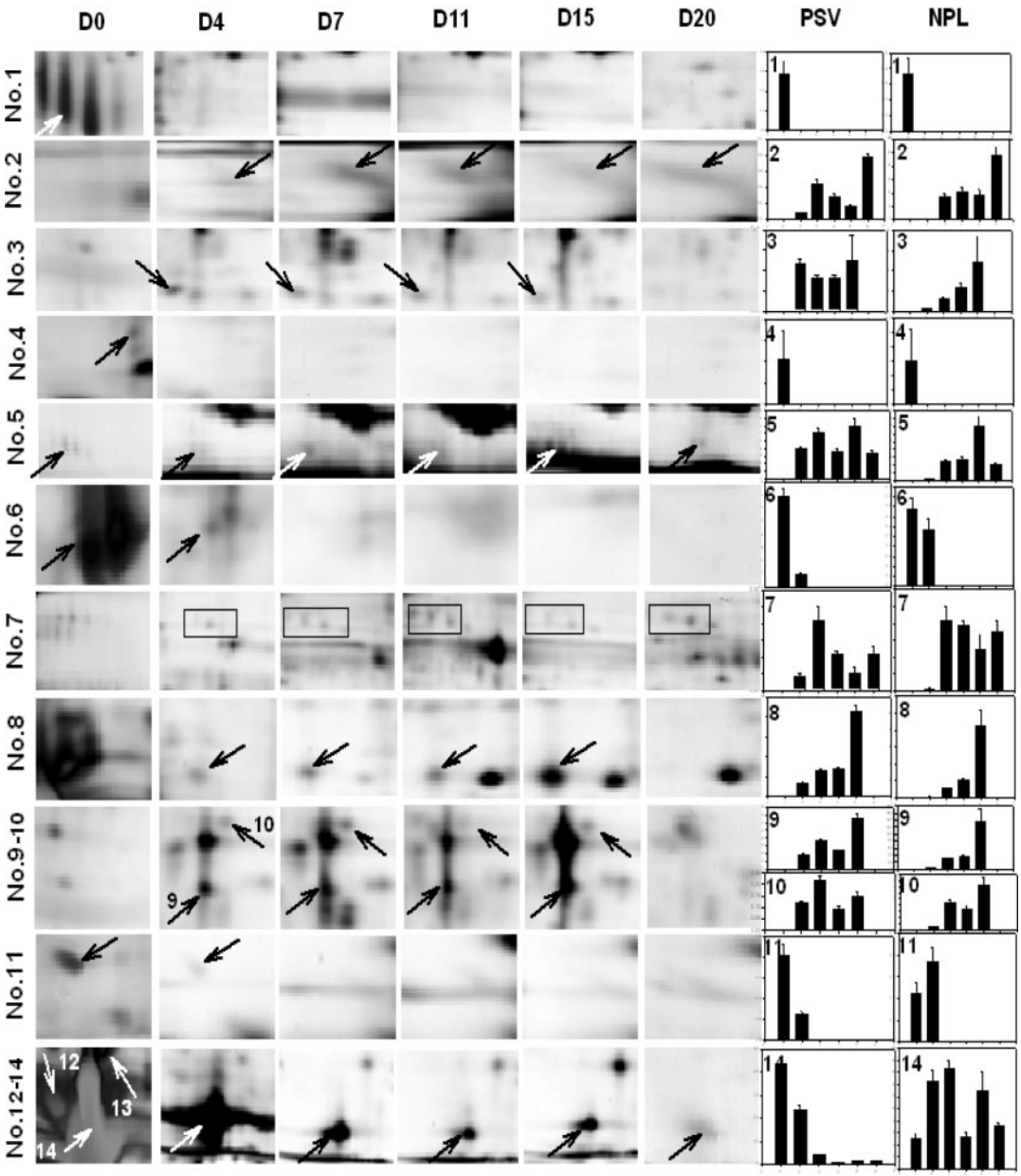

Fig. 5. Quantification of the PSV and NPL for identified proteins in the urine of AD-treated mice at different time points (day 0–day 20). The left six panels show magnified images of the local areas of the 2D gels containing the identified urinary proteins at different time points of FSGS. The boxes enclose spots assigned to the same protein. The right two panels show the statistical data ($n = 6$ for each day) for the PSV and NPL for the corresponding proteins. The PSV and NPL were calculated as described in the 'Subjects and methods' section. The *x*-axis indicates the day and the *y*-axis the PSV or NPL; the scale on the *y*-axis varies for different proteins.

family of proteins, which contain metalloprotease domain that cleaves ECM proteins [22], increased in the urine of the diseased mice (Figure 5).

Proteins associated with haemodynamic problems, oxidative stress, apoptosis and epithelial cell damage

Haemodynamic problems play a pathogenic role in FSGS. Kallikrein, which exerts a hypotensive function by converting kininogen into the vasoactive peptides, was detected in our 2D gels, in which kallikrein (spot 6, Table 1) was down-regulated, while kininogen precursor (spot 7, Table 1) was up-regulated, in urine of diseased mice (Figure 5). The other well-known cause of FSGS is the rise of oxidative stress that induces podocyte apoptosis. In our 2D gels, one anti-oxidation enzyme, the glutathione s-transferase (spot 8, Table 1) and two apoptosis-inducing proteins, the apoptosis-inducing factor-2 (AIF-2) (spot 9, Table 1) and annexin A1 (spot 10, Table 1), were increased, whereas the epithelial cell marker E-cadherin, (spot 11) was decreased in the urine of diseased mice (Figure 5). These changes match the oxidative stress and apoptosis mechanisms in FSGS pathogenesis.

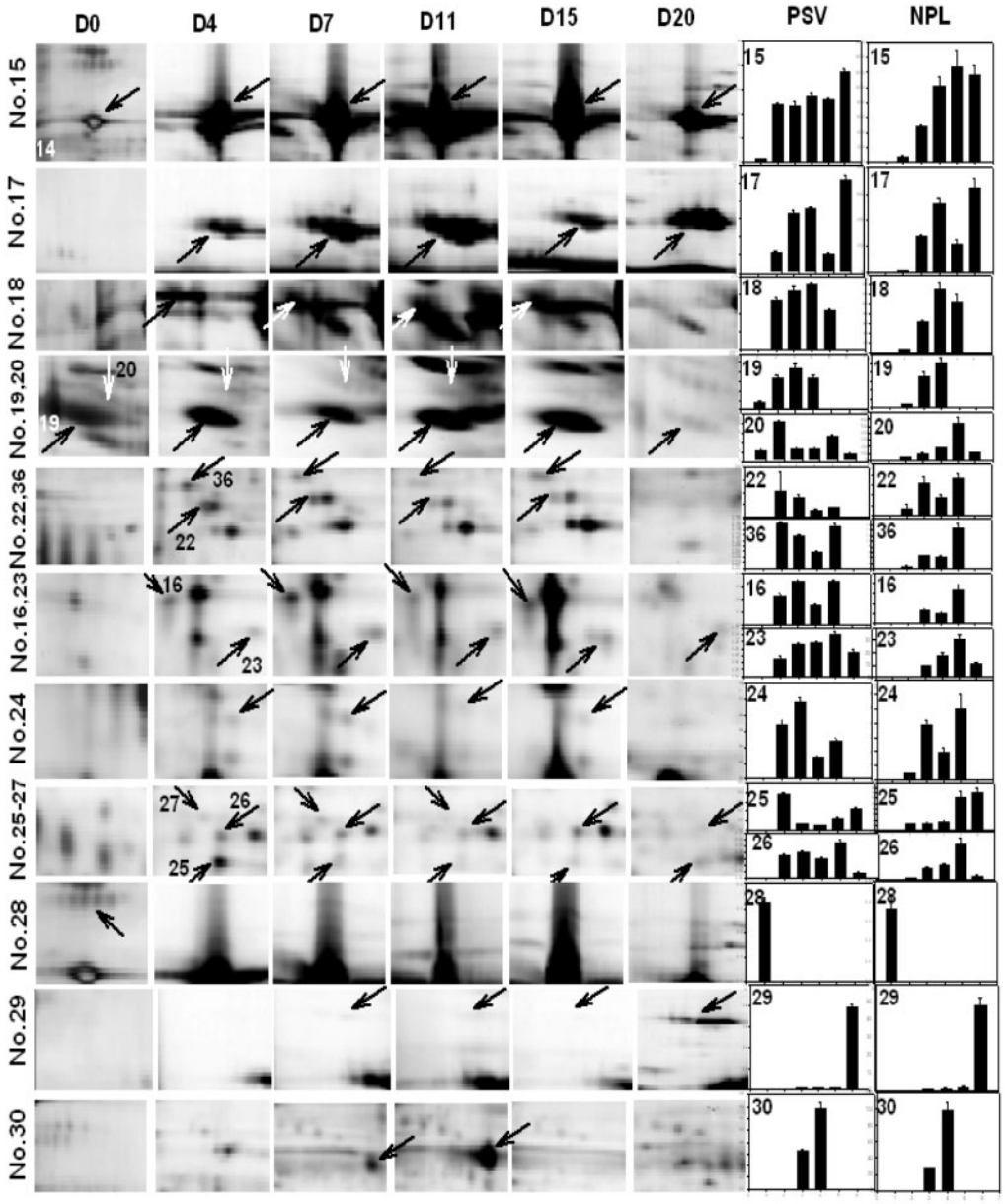

Fig. 5. Continued.

Discussion

Although proteinuria is a common phenomenon for different types of nephrotic syndromes, a previous proteomic study in patients has demonstrated that different nephrotic syndromes display different patterns of plasma proteins in urine, probably caused by disease-specific changes of glomerular permeability [11]. Some of the plasma proteins, including albumin (spot 15), transferrin (spot 17), α-1 anti-trypsin (spot 20) and plasma retinol-binding protein (spot 31) were also observed in our 2D gels.

In addition to the common plasma proteins, several novel urinary proteins with potential pathogenic roles in FSGS were identified in the present proteomic study. FSGS is characterized by proteinuria at the early stage and by glomerular sclerosis at the later stages. Haemodynamic problems and oxidative stress contribute to the proteinuria by enhancement of glomerular filtration rate and damage of podocytes respectively, while disturbed metabolism of ECM proteins and dysregulation of sclerotic factors lead to the glomerular sclerosis [1,2].

Glomerular haemodynamics, which is regulated by both the renin–angiotensin and kallikrein–kinin systems, is one of the factors causing proteinuria. The renin–angiotensin system increases blood pressure and affects the glomerular filtration rate; it is activated in the glomeruli in a renal-ablation rat FSGS model, associated with hyperperfusion, hyperfiltration and dysfunction of glomeruli [2,23]. Suppression of the system by angiotensin-converting enzyme inhibitors

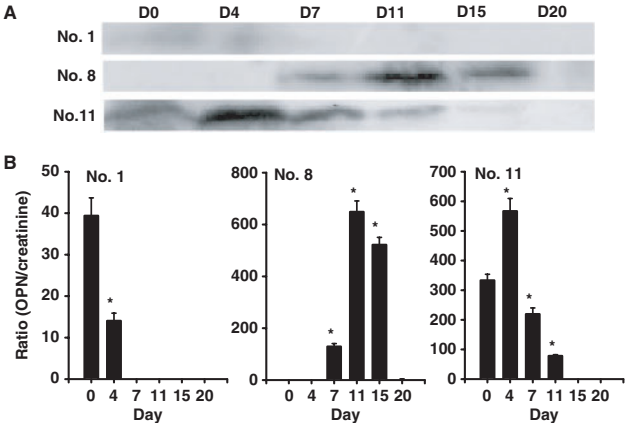

Fig. 6. Western blot analyses. (**A**) A representative Western blot analysis of collagen IV fragment (spot 1), glutathione S-transferase (spot 8) and E-cadherin (spot 11) in urine of mice taken at the indicated times. (**B**) Changes in the protein levels normalized to the corresponding urine creatinine levels. FSGS mice revealed increased excretion of glutathione s-transferase, and decreased excretion of collagen IV fragment and E-cadherin into urine. $^{*}P < 0.05$ compared to day 0.

can ameliorate FSGS in patients [24]. On the contrary, the kallikrein–kinin system, which decreases blood pressure and glomerular filtration by kallikrenin-mediated conversion of kininogen into vasodilator kinin, plays a beneficial role in glomerulosclerosis [25]. Imbalance between the renin–angiotensin and kallikrein–kinin systems usually leads to a diseased state [26]. Since our results showed a suppression of the kallikrein–kinin system, i.e. the kallikrein (spot 6) was decreased and its substrate kininogen (spot 7) increased in the diseased mice, a predominance of the renin–angiotensin system that causes proteinuria could be predicted.

Proteinuria in FSGS is also caused by the disruption of glomerular filtration barrier by oxidative stress-induced damage and/or apoptosis of podocytes [2,27,28]. Changes of several urinary proteins in our 2D gels could reflect the involvement of the mechanisms in FSGS. Consistent with a previous observation in diabetes nephropathy [29], the glutathione s-transferase (spot 8) in the diseased mice was up-regulated, representing a protective response against the AD-induced oxidative stress in FSGS. In addition, two apoptosis-inducing factors, AIF-2 and annexin A1, were increased in the urine of the diseased mice, the former being a novel protein that was demonstrated to play a key role in podocyte apoptosis in a caspase-independent manner [30]. Furthermore, in accordance with a proteomic report in membraneous nephropathy [10], E-cadherin (spot 11), an epithelial cell marker, was reduced in urine of the diseased mice, indicating a significant death of podocytes or other renal epithelial cells upstream.

Sclerosis that distorts the fine structure of glomeruli is a key feature of FSGS and a determinant of exacerbation of the disease. Glomerular sclerosis is caused by abnormal accumulation of ECM proteins. Although some of the deposited ECM proteins in glomeruli come from the blood during the initial stage of FSGS [15], most of the ECM proteins in the sclerosis are produced locally by glomerular cells [15,31,32]. In terms of metabolism, either enhanced synthesis of ECM proteins, such as collagen IV and fibronectin [15,32], or suppressed degradation of the proteins due to the down-regulation of proteinases [33], contributes to the sclerosis formation. Urinary collagen fragments are the products of collagen degradation, and have been suggested to serve as biomarkers for some basement membrane disorders [34]. The decreased excretion of collagen fragment observed in the diseased mice (spot 1) might be caused by suppressed degradation of intact collagen in the glomeruli, leading to collagen accumulation in FSGS [33].

Synthesis of ECM proteins is positively controlled by sclerotic factors, such as TGF-β and negatively regulated by anti-sclerotic factors, such as BMP-7. TGF-β stimulates ECM synthesis through the SMAD signalling pathway [21,35], and TGF-β up-regulation plays pathogenic roles in FSGS [36]; on the contrary, BMP-7 counteracts sclerosis by suppressing SMAD signalling [21]. However, two novel BMP-binding proteins, the cerberus (spot 3) and tomoregulin (spot 4), that suppress BMP activity [37] were identified in mouse urine in the present study. The increase of cerberus and decrease of tomoregulin fragment (reduced degradation of intact tomoregulin protein) in the diseased mice might indicate an inhibition of BMP activity which can cause predominance of the TGF-β sclerotic over the BMP-7 anti-sclerotic systems.

ECM 1 is a novel ECM protein never being reported to be associated with FSGS. ECM 1 causes two skin diseases, lipoid proteinosis and lichen sclerosus [38,39], due respectively to mutation of the gene and autoantibody targeting of the protein. In our proteomic results, ECM 1 excretion into urine was enhanced in FSGS mice. The role of ECM 1 in FSGS is unclear, but ECM1 might be involved in the pathogenesis of glomerular sclerosis, as lichen sclerosus, like FSGS, is a sclerotic disorder [39]. ECM 1 could have potential to serve as a novel biomarker of FSGS.

ADAM 32, a novel member of the ADAM family of proteins, contains a disintegrin domain that modulates the cell–ECM interaction and a metalloprotease domain that cleaves ECM proteins [22]. In the kidney, ADAM is up-regulated during chronic renal allograft rejection, and it has been shown to promote mesangial cell migration, enhance ECM protein degradation, and affect TGF-α action and glomerular sclerosis [40–43]. Accordingly, the increased levels of ADAM 32 in the urine of the diseased mice suggest a pathogenic role of ADAM 32 in FSGS.

In conclusion, 37 urinary proteins showing characteristic patterns of dynamic changes along the course of FSGS have been identified in the present proteomic study. Importantly, 11 proteins (spots 1–11) are novel to FSGS, and have known functions potentially involved in different steps of FSGS pathogenesis,

i.e. haemodynamic disturbance, podocyte apoptosis, ECM-protein deposition and sclerosis. We suggest that these novel proteins have potential to serve as non-invasive biomarkers for diagnosis and prognosis of FSGS, and give an insight into the pathogenic mechanisms of the disease.

Acknowledgements. This work was supported by grants NSC 93-2314-B-016-066 and NSC 95-2320-B-016-025 from the National Science Council.

Conflict of interest statement. None declared.

References

1. Benchimol C. Focal segmental glomerulosclerosis: pathogenesis and treatment. *Curr Opin Pediatr* 2003; 15: 171–180
2. Fogo AB. Animal models of FSGS: lessons for pathogenesis and treatment. *Semin Nephrol* 2003; 23: 161–171
3. Xu BJ, Shyr Y, Liang X *et al*. Proteomic patterns and prediction of glomerulosclerosis and its mechanisms. *J Am Soc Nephrol* 2005; 16: 2967–2975
4. Haubitz M, Wittke S, Weissinger EM *et al*. Urine protein patterns can serve as diagnostic tools in patients with IgA nephropathy. *Kidney Int* 2005; 67: 2313–2320
5. Cutler P, Bell DJ, Birrell HC *et al*. An integrated proteomic approach to studying glomerular nephrotoxicity. *Electrophoresis* 1999; 20: 3647–3658
6. Mosley K, Tam FW, Edwards RJ, Crozier J, Pusey CD, Lightstone L. Urinary proteomic profiles distinguish between active and inactive lupus nephritis. *Rheumatology* 2006; 45: 1497–1504
7. Park MR, Wang EH, Jin DC *et al*. Establishment of a 2-D human urinary proteomic map in IgA nephropathy. *Proteomics* 2006; 6: 1066–1076
8. Thongboonkerd V, Klein JB, Jevans AW, McLeish KR. Urinary proteomics and biomarker discovery for glomerular diseases. *Contrib Nephrol* 2004; 141: 292–307
9. Weissinger EM, Wittke S, Kaiser T *et al*. Proteomic patterns established with capillary electrophoresis and mass spectrometry for diagnostic purposes. *Kidney Int* 2004; 65: 2426–2434
10. Ngai HH, Sit WH, Jiang PP, Xu RJ, Wan JM, Thongboonkerd V. Serial changes in urinary proteome profile of membranous nephropathy: implications for pathophysiology and biomarker discovery. *J Proteome Res* 2006; 5: 3038–3047
11. Varghese SA, Powell TB, Budisavljevic MN *et al*. Urine biomarkers predict the cause of glomerular disease. *J Am Soc Nephrol* 2007; 18: 913–922
12. Teschner M, Schaefer RM, Paczek L, Heidland A. Effect of renal disease on glomerular proteinases. *Miner Electrolyte Metab* 1992; 18: 92–96
13. Woroniecki RP, Schiffer M, Shaw AS, Kaskel FJ, Bottinger EP. Glomerular expression of transforming growth factor-beta (TGF-beta) isoforms in mice lacking CD2-associated protein. *Pediatr Nephrol* 2006; 21: 333–338
14. Chen A, Sheu LF, Ho YS *et al*. Experimental focal segmental glomerulosclerosis in mice. *Nephron* 1998; 78: 440–452
15. Shui HA, Ka SM, Lin JC *et al*. Fibronectin in blood invokes the development of focal segmental glomerulosclerosis in mouse model. *Nephrol Dial Transplant* 2006; 21: 1794–1802
16. Shui HA, Ka SM, Yang SM, Lin YF, Chen A. Osteopontin as an injury marker expressing in epithelial hyperplasia lesions helpful in prognosis of focal segmental glomerulosclerosis. *Transl Res* 2007 (in press)
17. Shui HA, Ho ST, Wang JJ *et al*. Proteomic analysis of spinal protein expression in rats exposed to repeated intrathecal morphine injection. *Proteomics* 2007; 7: 796–803
18. Ramagli LS. Quantifying protein in 2-D PAGE solubilization buffer. In: Link, AJ (ed). *2-D Proteome analysis protocols*. Totowa, NJ: Humana Press, 1999; 99–103
19. Montinaro V, Hevey K, Aventaggiato L *et al*. Extrarenal cytokines modulate the glomerular response to IgA immune complexes. *Kidney Int* 1992; 42: 341–353
20. Tantipaiboonwong P, Sinchaikul S, Sriyam S, Phutrakul S, Chen ST. Different techniques for urinary protein analysis of normal and lung cancer patients. *Proteomics* 2005; 5: 1140–1149
21. Whitman M, Mercola M. TGF-beta superfamily signaling and left-right asymmetry. *Sci STKE* 2001; 2001: RE1
22. Primakoff P, Myles DG. The ADAM gene family: surface proteins with adhesion and protease activity. *Trends Genet* 2000; 16: 83–87
23. Correa-Rotter R, Hostetter TH, Manivel JC, Rosenberg ME. Renin expression in renal ablation. *Hypertension* 1992; 20: 483–490
24. Stiles KP, Abbott KC, Welch PG, Yuan CM. Effects of angiotensin-converting enzyme inhibitor and steroid therapy on proteinuria in FSGS: a retrospective study in a single clinic. *Clin Nephrol* 2001; 56: 89–95
25. Pawluczyk IZ, Patel SR, Harris KP. The role of bradykinin in the antifibrotic actions of perindoprilat on human mesangial cells. *Kidney Int* 2004; 65: 1240–1251
26. Shen B, El-Dahr SS. Cross-talk of the renin-angiotensin and kallikrein-kinin systems. *Biol Chem* 2006; 387: 145–150
27. Shiiki H, Sasaki Y, Nishino T *et al*. Cell proliferation and apoptosis of the glomerular epithelial cells in rats with puromycin aminonucleoside nephrosis. *Pathobiology* 1998; 66: 221–229
28. Wang W, Tzanidis A, Divjak M, Thomson NM, Stein-Oakley AN. Altered signaling and regulatory mechanisms of apoptosis in focal and segmental glomerulosclerosis. *J Am Soc Nephrol* 2001; 12: 1422–1433
29. Fujita H, Haseyama T, Kayo T *et al*. Increased expression of glutathione S-transferase in renal proximal tubules in the early stages of diabetes: a study of type-2 diabetes in the Akita mouse model. *Exp Nephrol* 2001; 9: 380–386
30. Wada T, Pippin JW, Marshall CB, Griffin SV, Shankland SJ. Dexamethasone prevents podocyte apoptosis induced by puromycin aminonucleoside: role of p53 and Bcl-2-related family proteins. *J Am Soc Nephrol* 2005; 16: 2615–2625
31. Bergijk EC, Baelde HJ, de Heer E, Killen PD, Bruijn JA. Role of the extracellular matrix in the development of glomerulosclerosis in experimental chronic serum sickness. *Exp Nephrol* 1995; 3: 338–347
32. Razzaque MS, Koji T, Harada T, Nakane PK, Taguchi T. Primary focal segmental glomerulosclerosis is associated with increased intraglomerular type IV collagen synthesis. *Clin Chim Acta* 1995; 235: 121–124
33. Ahuja TS, Gopalani A, Davies P, Ahuja H. Matrix metalloproteinase-9 expression in renal biopsies of patients with HIV-associated nephropathy. *Nephron Clin Pract* 2003; 95: c100–c104
34. Bowman BH, Schneider L, Barnett DR, Kurosky A, Goldblum RM. Novel urinary fragments from human basement membrane collagen. *J Biol Chem* 1980; 255: 9484–9489
35. Docherty NG, Perez-Barriocanal F, Balboa NE, Lopez-Novoa JM. Transforming growth factor-beta1 (TGF-beta1): a potential recovery signal in the post-ischemic kidney. *Ren Fail* 2002; 24: 391–406
36. Kim JH, Kim BK, Moon KC, Hong HK, Lee HS. Activation of the TGF-beta/Smad signaling pathway in focal segmental glomerulosclerosis. *Kidney Int* 2003; 64: 1715–1721
37. Chang C, Eggen BJ, Weinstein DC, Brivanlou AH. Regulation of nodal and BMP signaling by tomoregulin-1 (X7365) through novel mechanisms. *Dev Biol* 2003; 255: 1–11
38. Hamada T, McLean WH, Ramsay M *et al*. Lipoid proteinosis maps to 1q21 and is caused by mutations in the extracellular

matrix protein 1 gene (ECM1). *Hum Mol Genet* 2002; 11: 833–840
39. Oyama N, Chan I, Neill SM *et al.* Autoantibodies to extracellular matrix protein 1 in lichen sclerosus. *Lancet* 2003; 362: 118–123
40. Berthier CC, Lods N, Joosten SA *et al.* Differential regulation of metzincins in experimental chronic renal allograft rejection: potential markers and novel therapeutic targets. *Kidney Int* 2006; 69: 358–368
41. Martin J, Eynstone LV, Davies M, Williams JD, Steadman R. The role of ADAM 15 in glomerular mesangial cell migration. *J Biol Chem* 2002; 277: 33683–33689
42. Shah BH, Catt KJ. TACE-dependent EGF receptor activation in angiotensin-II-induced kidney disease. *Trends Pharmacol Sci* 2006; 27: 235–237
43. Roy R, Wewer UM, Zurakowski D, Pories SE, Moses MA. ADAM 12 cleaves extracellular matrix proteins and correlates with cancer status and stage. *J Biol Chem* 2004; 279: 51323–51330

Received for publication: 23.5.07
Accepted in revised form: 30.7.07